

Resilience of urban rail networks globally guided by mesoscale and connectivity attributes

Orijeet Mukherjee^{1,2}, Dongqin Zhou^{1,2}, Ashis Pal¹,
Jack Watson^{1,4}, Marta Gonzalez³, Samrat Chatterjee⁴,
Auroop Ganguly^{1,2,4*}

¹Sustainability and Data Sciences Laboratory, Northeastern University,
Boston, 02115, MA, USA.

²AI for Climate and Sustainability, Institute for Experiential AI,
Boston, 02115, MA, USA.

³Department of City and Regional Planning, University of California,
Berkeley, Berkeley, 94720, California, USA.

⁴Pacific Northwest National Laboratory, Richland, 99352, WA, USA.

*Corresponding author(s). E-mail(s): a.ganguly@northeastern.edu;
Contributing authors: mukherjee.o@northeastern.edu;
d.zhou@northeastern.edu; ashispalrny@gmail.com;
watson.jac@northeastern.edu; martag@berkeley.edu;
samrat.chatterjee@pnnl.gov;

Abstract

Urban metro rail systems are crucial lifelines that play key roles in mobility, accessibility, economic activity, serving millions daily. However, they are vulnerable to a range of natural and human induced disruptions. In this study, we simulate 7 different failure and recovery scenarios in a set of 45 global metro networks around the world to examine how network topology influences resilience. Existing studies seldom integrate varied failure/recovery strategies and topology at cross system scale. Our analysis of 25 network attributes, their interaction, and collective behavior reveal their influence on fragility and restoration. Our findings indicate that a consistent set of grouped attributes may be particularly crucial in identifying vulnerabilities and improving resilience. These insights have practical value for transport infrastructure design, retrofitting, emergency management, and urban planning. We demonstrate the value of these global insights by retrofitting Boston's metro, improving failure resilience and accelerating recovery through targeted topological interventions.

Keywords: Resilience, Network Science, Disruption, Restoration, Infrastructure, Metro, Complex Networks

Urban metro systems are vital to the daily functioning of modern cities—facilitating the movement of millions and underpinning economic and social activities. Their vulnerability to multi hazard disruptions from natural disasters to cyber physical attacks poses increasing challenges in the context of global environmental change and geopolitical tensions[1, 2]. While prior work has explored resilience in specific metro systems, most have focused on limited networks, isolated strategies, or a narrow set of topological attributes[3–5]. There is a need for a unified framework that systematically evaluates how different failure and recovery interventions interact with structural features across diverse global contexts. We address that problem by going across 45 urban rail systems, comparing 7 disruption and restoration strategies through simulations studying over 25 structural network attributes. We find that failure resilience is governed by global efficiency metrics, betweenness centrality distribution, and modularity patterns while recovery depends more on loop structures and degree inequality metrics. By translating complex network science into actionable planning insights for data driven retrofitting and design of rail systems. This work informs multi objective resilience planning, enabling cities to prioritize retrofits based on both systemic vulnerabilities and post disruption restoration capacity[6, 7].

Resilience in the context of urban metro systems extends beyond engineering robustness. It reflects a city’s capacity to maintain some of its most essential mobility functions and recover efficiently from disruptions. As cities increasingly rely on public transport for accessible and sustainable mobility, ensuring reliable metro operations is a critical aspect of urban resilience. A single targeted failure in a key metro node can spread through interconnected systems, not only affecting commuters but also affecting emergency response, commerce, and energy usage patterns[5]. In an era marked by intensification of climate extremes, cyber vulnerabilities, and geopolitical uncertainties, resilience has become a practical necessity to safeguard critical urban infrastructure[8, 9]. High profile incidents from cyberattacks targeting transport signaling systems to localized flooding disrupting major underground stations, highlight the need to prepare metro networks for diverse and compound threats. These events reveal how adversarial actors can exploit the structural and operational interdependencies of rail networks to create significant societal disruption[10].

Recent studies demonstrate that resilience is both measurable and actionable. For example, Pagani et al.[11] identified topological vulnerabilities and cascade dynamics across various networks, while Xu et al.[12] examined how interdependence between metro and bus systems affects functionality under stress. Structural studies using motif analysis reveal how recurring subgraph patterns can enhance rerouting capacity during disruptions[6]. Real world cases further illustrate these principles: London’s Central Line disruption in 2015 caused widespread congestion due to reliance on key transfer hubs, while Tokyo’s multi loop metro design facilitated faster recovery after the 2011 earthquake[13, 14]. These examples highlight the value of moving beyond localized solutions toward network strategies informed by complex network science. This study

contributes to an evolving framework for cities to anticipate vulnerabilities and guide infrastructure resilience[15].

Resilience in metro systems is increasingly assessed through both structural and dynamic metrics. A common indicator is the Area Under the Performance Curve (AUC), which captures both the rate of degradation during failure and the efficiency of recovery over time[16]. Complementary robustness measures, such as centrality based dismantling, assess how quickly the largest connected component breaks down, exposing structural vulnerabilities. Where operational data is available, researchers have also incorporated spatiotemporal accessibility metrics to account for service equity. The Generalized Travel Cost (GTC), which includes factors like in vehicle time, waiting, and transfers, offers a user centered view of network performance and helps prioritize interventions that minimize overall travel burden during crises[17]. Some existing models are highly localized—relying on city specific passenger data. In contrast, our approach focuses on deriving resilience insights directly from network topology, making it possible to identify critical trends and patterns without dependence on localized data, enhancing scalability.

Figure 1 illustrates the geographic and structural scope of our study. Figure 1a maps the locations of all 45 metro systems analyzed, with six major networks: Buenos Aires, Tokyo, San Francisco, New York, Paris, and Delhi. The are zoomed in to underscore their real world exposure to critical disruptions, including derailments, terrorist attacks, power outages, and sabotage. These include the 2012 Buenos Aires rail crash[18], the 1995 Tokyo subway sarin attack[19], the 1939 City of San Francisco derailment[20], the 2024 NYC subway power failure[21], the coordinated sabotage of Paris’s train network ahead of the Olympic[22], and the 2008 serial bomb blasts near Delhi metro stations[23]. The annotations also display each system’s annual ridership (in millions), reinforcing the high societal, economic, and operational stakes involved. Figure 1b presents the corresponding network attributes used in our analysis. To ground our analysis in established knowledge, we reviewed 21 influential papers in the domain of urban rail resilience and complex networks. This effort led to the construction of a comprehensive and interpretable list of structural features—many of which have been recurrently cited across studies[3–6, 10, 17, 24–38] referenced in Extended Table A1. Beyond attributes tailored to rail infrastructure resilience (e.g., average degree, density, and meshedness coefficient), we also include general topological descriptors drawn from the broader network science literature—such as algebraic connectivity, degree variance etc (formulated in equation 3, 4, 5) thereby enriching the scope of our study.

1 Results

We simulate failures and recoveries using various intervention strategies described in Section 3 across all 45 urban metro rail networks. At each time step t of node removal or addition, we define the functionality of a metro network by the relative size of its

largest Giant Connected Component (GCC), as shown in Equation (1).

$$F(t) = \frac{G(t)}{G(0)} \quad (1)$$

Where $G(t)$ is the size of the largest GCC at time t , and $G(0)$ is the size of the original network's largest GCC before any perturbation. This approach, rooted in percolation theory, considers the GCC as a proxy for the network's ability to maintain connectivity under failure or attack. To evaluate the overall resilience of the network during a disruption or recovery process, we calculate the AUC of the functionality over time, defined in Equation (2).

$$R = \frac{1}{N} \int_{t_0}^{t_1} F(t) dt \quad (2)$$

Here, R denotes the resilience score of the network, defined as the normalized area under the performance curve over the course of a failure or recovery process. The function $F(t)$ represents the global network performance at step t , with t_0 indicating the start of the trajectory (before any intervention), t_1 denoting the end of the trajectory (when all nodes have been removed or restored), and N being the total number of steps (i.e., the number of nodes). This formulation captures the cumulative functionality maintained (or regained) across the full sequence of disruption and restoration. A higher value of this integral indicates that the network retains greater connectivity over the entire time span of the disruption or recovery process, reflecting greater resilience. Dividing it by N , the score is normalized, allowing for consistent and fair comparisons of resilience between networks of different sizes. This method has been widely adopted in resilience assessment studies [39], providing a standardized approach to quantify resilience across different network scenarios. To assess network resilience under different disruption and restoration conditions, we conducted simulation based experiments across all 45 urban metro networks. Each simulation includes two phases: (1) a targeted or random failure sequence, where nodes were progressively removed from the original network; and (2) a recovery sequence, where nodes were sequentially reintroduced into a fully failed network (Algorithms 1, 2, 3, 4, 5, 6). We evaluated five targeted approaches based on network centrality—**Domirank**[40], **Betweenness**, **Degree**, **Closeness**, and **Eigen vector**—and one optimization based i.e **Greedy** strategy and one random based i.e **Mean Random** strategy. These represent a comprehensive set of centrality based methods commonly used in the literature for network resilience analysis and they cover a range of perspectives on node importance, ensuring that the simulation captures diverse disruption and recovery dynamics. These strategies simulate varying forms of physical, cyber, or operational disruptions and interventions. The AUC was calculated for each trajectory as the resilience score, defined in Equation (2).

Extended Figure A1 shows examples of these simulation outcomes for three cities: New York, Stockholm, and Warsaw. Across both failure (Extended Figure A1 a,b,c) and recovery (Extended Figure A1 d,e,f). These three cities were selected as representative examples of large, medium, and small metro networks, respectively, within our

broader set of cities. The performance curves illustrate how different strategies produce varying degradation and recovery patterns. We repeated this process for all the metro networks and obtained resilience scores under each strategy.

Figure 2 presents the resilience scores—quantified as AUC—for all 45 networks under 7 different node intervention strategies. Figure 2a displays the degradation outcomes during failure simulations, while Figure 2b shows the corresponding recovery trajectories. Across the failure heatmap, the Greedy, Domirank, Betweenness, and Degree based strategies consistently lead to the most severe degradation, with the lowest average AUC scores across networks. In contrast, the Mean Random and Closeness based removals result in slower degradation. This pattern reinforces the idea that not all centralities are equally damaging—some (like Domirank) concentrate failure impact, while others (like Closeness or Mean Random) allow for a more gradual breakdown. On the recovery side, the most efficient restoration tends to occur under Domirank and Greedy while others yielding a comparatively slower recoveries.

With resilience scores computed for each of the metro networks under seven failure and recovery strategies, we then move towards understanding their relationship with topological attributes in the context of urban rail, we conducted a statistical analysis, 2D Kendall Tau [41] correlation plot, displayed in Figure 3, which confirms pronounced multicollinearity among the 25 structural attributes: nearly one third of all attribute pairs exceeding more 0.75 correlation score, and a few reach around 0.97. By flagging every pair above the 0.75 correlation threshold, we identify the subsets most likely to convey redundant information[42]. The pronounced multicollinearity we observe is rooted in real world engineering constraints: most of the urban railways must follow them which is the reason our urban metros look like the ones in panels Extended Figure A2a (Boston) and Extended Figure A2b (Delhi) rather than the highly entangled, Erdős–Rényi meshes in panels Extended Figure A2c and Extended Figure A2d, whose attribute combinations are physically unattainable for metro construction.

To probe this redundancy we begin by constructing a dissimilarity matrix from Kendall's Tau correlations, defined as one minus the absolute Kendall's Tau value for each attribute pair. In this formulation of the dissimilarity matrix, smaller numbers indicate pairs of attributes that are highly correlated and thus more similarity, while larger numbers indicate weaker correlation and greater dissimilarity. Using this dissimilarity matrix, we then apply Metric Multidimensional Scaling (MDS) [43] to embed the attributes into a two-dimensional latent space displayed in Figure 4. The resulting axes are unitless and carry no physical meaning, MDS preserves only the relative distances between attributes, such that strongly correlated variables appear close together while uncorrelated ones are positioned farther apart. To highlight strong relationships, we connect pairs of attributes with an edge whenever their absolute Kendall's Tau exceeds 0.75, forming a network of associations. We get 9 nine distinct connected components which, we call as clusters. Each representing a group of attributes that emit similar structural signals. These clusters are assigned unique colors in the Figure 4, providing an interpretable visualization of how groups of network attributes align or diverge in the resilience analysis.

Another metric we bring into the study is Mutual Information [44]. Unlike traditional correlation metrics, Mutual Information captures both linear and nonlinear

dependencies, making it inherently robust to multicollinearity. This approach is well suited for identifying network attributes that provide the most informative signal about resilience, even when their influence is masked by interdependencies[44, 45]. Mutual information between each attribute and the resilience scores for failures are shown in Figure 5a and for recovery in Figure 5b. Darker greens highlight the attributes that deliver the largest unique signal. We deliberately omit the eigenvector and closeness centrality based failures in the failure heatmap as their mutual information scores with network attributes exhibit little to no variation as shown in Figure A3, indicating that the resilience outcomes these two produce are largely insensitive to underlying topology and therefore add little explanatory value. To isolate the most informative variables we retain only attributes whose mutual information scores lie above the seventy fifth percentile for each context. Extended Figure A4 plots the full mutual information distributions for failure and recovery; the red dashed lines mark the respective cut off values (0.35 for failure, 0.28 for recovery). Attributes to the right of these thresholds constitute the “strong signal” allowing us to focus on the drivers that contribute genuine explanatory power while filtering out noise from weaker, statistically unreliable metrics.

Building on the mutual information filtering and cluster definitions, Extended Figure A5 synthesizes how these high signal attribute clusters are distributed across individual strategies, while Extended Table A2 complements this by explicitly listing which clusters uniquely appear above the threshold for each strategy. Extended Figure A5a shows that for failure resilience, Cluster 1—dominated by connectivity, efficiency, and size metrics—appears most frequently, followed by Cluster 5 (average betweenness centrality) and Cluster 4 (modularity index). Extended Table A2 confirms this dominance, showing Cluster 1’s consistent presence across almost all failure strategies, with Clusters 4 and 5 appearing more selectively, highlighting strategies that exploit modularity index or high average betweenness based routing advantages. This aligns with our interpretation that denser networks with stronger global connectivity can better withstand node removals, while high average betweenness centrality enables alternate routing, and low modularity avoids the rapid GCC collapse typical in modular networks when hubs are targeted. It is important to note that here we refer to the high average betweenness of the entire network to make it more resilient, not high betweenness concentrated in one or a few nodes, as such concentration would increase vulnerability to hub based attacks instead of reducing it.

Extended Figure A5b, along with the recovery portion of Extended Table A2, shows a different emphasis: Cluster 8 captures degree heterogeneity and inequality emerges most frequently, with Clusters 1 and 9 (showing betweenness inequality) also recurring, and Cluster 2 (average degree, loops, meshedness) contributing in several strategies. Here, recovery performance appears more tied to loop based and degree distribution driven properties that promote reconnection efficiency. Extended Table A2 further shows that Clusters 8 and 2 often co occur in recovery strategies; given their close proximity in the semantic attribute space in Figure 4, this suggests they convey similar resilience signals. A similar spatial closeness exists between Clusters 5 and 9, indicating that their contribution to recovery behaviour is also related. Hence, it confirms that closely positioned clusters in the semantic map often represent overlapping resilience

guiding signals, reinforcing the importance of redundancy analysis and cluster based dimensionality reduction in resilience modelling.

Failure resilience is strongest in networks that are dense, globally connected, and less modular, as such structures degrade more gradually and allow alternate routing through high betweenness pathways, whereas recovery resilience depends more on degree heterogeneity and loop redundancy, which together enable efficient reconnection and rapid restoration of performance. We repeated the entire process by excluding Boston and analyzing the remaining 44 metro systems, obtaining consistent findings as for the entire set of 45. These insights were then translated into a retrofitting plan for Boston's metro, shown in Figure 6a for the physical placement of edges used in failure resilience analysis and Figure 6b for those used in recovery resilience analysis. We use the Domirank failure and recovery strategies, as Domirank has been identified in the literature as one of the most effective network dismantling approaches, and its novel application to urban rail systems makes it the most suitable candidate for our retrofitting test case. In the failure focused retrofit, the added edges (in red) link structurally, bridging major lines and peripheral segments to bypass singular high betweenness hubs and reduce over reliance on central bottlenecks. This directly reflects our failure resilience findings that denser, better connected networks with reduced centrality concentration are more robust under DomiRank failure, particularly when modularity is low enough to prevent catastrophic giant connected component collapse. In the recovery focused retrofit, connections were chosen to increase loops and balance degree distribution, aligning with our recovery analysis. Performance results confirm the practical value of this topology aware approach, with Figure 6c showing an 11.9% improvement in failure AUC and Figure 6d showing a 3% gain in recovery AUC over random edge addition with 95% confidence interval (CI) with 50 trials per strategy. The sets of edges selected for retrofitting differ between failure and recovery, reflecting the inherently distinct dynamics of degradation and restoration. By applying a topological lens to the problem of metro resilience, we moved beyond abstract simulation outputs to design spatially grounded retrofitting strategies that directly target the structural weaknesses revealed by our attribute–cluster and mutual information analyses. This approach demonstrates that resilience gains can be systematically engineered by leveraging the intrinsic connectivity patterns of urban rail networks, translating network science insights into concrete, geographically actionable interventions.

2 Discussion

Reflecting on how our analysis of attribute interactions, combined with mutual information based insights, advances the understanding of metro network resilience. By systematically disentangling redundancy, identifying high signal network attribute clusters, and validating their role through targeted retrofitting experiments, we demonstrate a pathway to address several persistent challenges in resilience research —namely, the difficulty of isolating actionable design levers in the presence of strong multicollinearity, and the translation of abstract network metrics into spatially and operationally viable interventions. Our findings reinforce the view that resilience is an

outcome shaped by the interplay of topological attributes, positioning topological analytics as a tool for guiding urban rail infrastructure planning and adaptation strategies in the face of diverse hazards. The 25 structural attributes we analyzed—spanning 45 urban rail systems across five continents and evaluated under seven failure and seven recovery strategies form the core of our resilience assessment, making this study one of the most comprehensive comparative evaluations of metro networks to date. Crucially, it is among the first to integrate DomiRank Centrality, a recent advancement in centrality theory, into the urban rail context. Our approach is also significantly more computationally and resource efficient compared to certain data heavy methods discussed in [17], which require extensive simulation time—often several hours—to generate results. In contrast, our methodology relies on easily computable network metrics, such as density, modularity, and centrality, allowing for resilience assessments in seconds or minutes. This efficiency does not come at the expense of accuracy; the results align with established findings in the literature, providing a strong basis for advancing resilience analysis [6, 17, 26, 29].

To further enhance the practical utility of this line of work, several directions merit investigation. Incorporating temporal dynamics into disruption and recovery modeling can substantially enhance resilience assessments. Time dependent network analysis has proven useful for simulating realistic disruption scenarios and prioritizing recovery efforts [46, 47]. Embedding such dynamics into our framework would allow stakeholders to better prepare for cascading failures and delays in urban infrastructure systems. Moreover, expanding this interpretability driven methodology to multimodal transport systems—combining metros with buses, trams, and other modes—could provide a more holistic understanding of urban resilience. Multilayer network approaches have shown promise in modeling these interdependencies and uncovering new strategic levers for resilience planning [48]. Future research could also explore the development of a parameterized approximation function, where resilience is expressed as a tractable function of selected network attributes, enabling rapid plug and play estimates once larger datasets or orthogonalized features mitigate current limitations. Additionally, testing the transferability of our study to other infrastructure domains, such as energy grids or water networks, could open the door to cross sector resilience diagnostics. Recent interdisciplinary studies demonstrate the value of such generalization [49]. This work serves as a step for simulation driven resilience analysis with transparent analytical modeling, equipping urban planners, engineers, and policymakers with insights to anticipate vulnerabilities and guide network design or retrofitting strategy.

3 Methods

Network Attributes

We consider several structural attributes that capture redundancy, variability, and heterogeneity in metro networks. Below we define three measures used in our analysis:

- **Normalized Number of Loops**

$$\text{Normalized Number of Loops} = \frac{L}{N} \quad (3)$$

where L denotes the total number of independent cycles (loops) in the undirected network, and N is the number of nodes. This ratio reflects the level of redundancy relative to network size.

- **Coefficient of Variation**

$$\text{Coefficient of Variation} = \frac{\sigma_k}{\mu_k} \quad (4)$$

where σ_k is the standard deviation of node degree and μ_k is the mean node degree. It measures the relative variability in connectivity across stations.

- **Degree Variance**

$$\text{Degree Variance} = \frac{1}{N} \sum_{i=1}^N (k_i - \mu_k)^2 \quad (5)$$

where k_i is the degree of node i , and μ_k is the average degree of the network. This captures the absolute spread of node connectivity within the system.

Failure and Recovery

To evaluate the resilience of urban metro networks, we simulate both failure and recovery phases using a node level intervention process. In the failure phase, the simulation begins from the fully intact, undamaged network and proceeds toward complete collapse, as nodes (stations) are sequentially removed according to a given strategy—such as a centrality based ranking or a randomly generated permutation. At each step of node removal, the global network performance is computed to track the progressive degradation in functionality until the network is fully dismantled and connectivity is lost.

In the recovery phase, the process runs in the opposite direction: starting from the completely dismantled state with no functional connectivity, the previously removed nodes are reintroduced one at a time along with their original edges, following a given strategy. This continues until the network is fully restored, allowing us to evaluate the effectiveness of each strategy in accelerating the restoration of functionality.

Centrality Measures

We evaluate seven node prioritization strategies—five based on well known centrality metrics in network science, and one based on random permutation and one based on greedy optimization technique. Each centrality score is computed on the initial graph structure and then used to order nodes for failure or recovery simulations.

- **Domirank:** A recent centrality measure that evaluates a node's dominance by considering both its direct influence and broader propagation effects in the network. Domirank captures how critical a node is in terms of its ability to control paths and substructures across the graph. For full formulation and methodological details, see [40].
- **Betweenness Centrality:** Measures the extent to which a node lies on shortest paths between other nodes. A high betweenness score implies that the node is a key

bridge within the network. It is defined as:

$$C_B(v) = \sum_{s \neq v \neq t} \frac{\sigma_{st}(v)}{\sigma_{st}}$$

where σ_{st} is the total number of shortest paths from node s to t , and $\sigma_{st}(v)$ is the number of those paths that pass through v .

- **Degree Centrality:** Counts the number of immediate connections (edges) a node has. For undirected graphs, it is simply:
- **Eigenvector Centrality:** Assigns relative scores to nodes based on the principle that connections to high scoring nodes contribute more to the score of the node in question. It is computed as the principal eigenvector of the adjacency matrix A :

$$A \cdot \vec{x} = \lambda \vec{x}$$

- **Closeness Centrality:** Measures the inverse of the average shortest path length from a node to all others in the network, capturing how close a node is to all others:

$$C_C(v) = \frac{1}{\sum_{t \neq v} d(v, t)}$$

where $d(v, t)$ is the shortest path distance between nodes v and t .

- **Mean Random:** Nodes are removed (or reintroduced) based on 50 independent random permutations. The performance curve from each run is collected, and the mean curve is taken as the final representative trajectory. Additionally, the 95% confidence interval is calculated across the runs to quantify variability and displayed in Extended figure A1
- **Greedy Strategy:** An optimization based approach that iteratively selects the next node for removal (or addition, in recovery) by evaluating the network wide performance impact of each candidate at every step. At each iteration, the node whose removal causes the largest drop in the Giant Connected Component (for failure) or whose addition yields the largest increase (for recovery) is chosen.

Kendall's Tau Rank Correlation

Kendall's Tau is a non parametric measure of association between two variables, based on the relative ordering of their observations. Given two network attribute X and Y with n paired observations, τ is defined as:

$$\tau(X, Y) = \frac{N_c - N_d}{\binom{n}{2}},$$

where N_c is the number of concordant pairs and N_d is the number of discordant pairs. Unlike Pearson correlation, Kendall's Tau does not assume a linear relationship or normally distributed data.

Dissimilarity Matrix and Metric Multidimensional Scaling

A dissimilarity matrix provides a pairwise measure of distance (dissimilarity matrix in our case) between attribute pairs. When Kendall's Tau is used as the similarity measure, the corresponding dissimilarity between attributes i and j can be defined as:

$$D_{ij} = 1 - |\tau_{ij}|,$$

where τ_{ij} is the Kendall correlation between attributes i and j .

MDS takes the dissimilarity matrix \mathbf{D} and finds a low dimensional configuration of points $\{\mathbf{z}_i\}$ that preserves these pairwise distances as closely as possible. The optimization problem can be expressed as:

$$\min_{\mathbf{z}_1, \dots, \mathbf{z}_m} \sum_{i < j} (\|\mathbf{z}_i - \mathbf{z}_j\|_2 - D_{ij})^2.$$

The resulting embedding enables visual exploration of attribute relationships: attributes with high correlation appear close together, while those with weak correlation appear farther apart.

Mutual Information

Mutual Information quantifies the amount of information shared between two random variables, capturing both linear and non linear dependencies. For variables X and Y with joint density $p_{X,Y}$ and marginals p_X, p_Y , it is defined as:

$$I(X; Y) = \iint p_{X,Y}(x, y) \log \frac{p_{X,Y}(x, y)}{p_X(x) p_Y(y)} dx dy.$$

A zero Mutual Information value indicates statistical independence, while higher values imply stronger dependence. When applied to feature selection, Mutual Information serves to rank attributes by their ability to explain variability in a target variable, helping to identify the most informative features while remaining robust to collinearity.

4 Figures

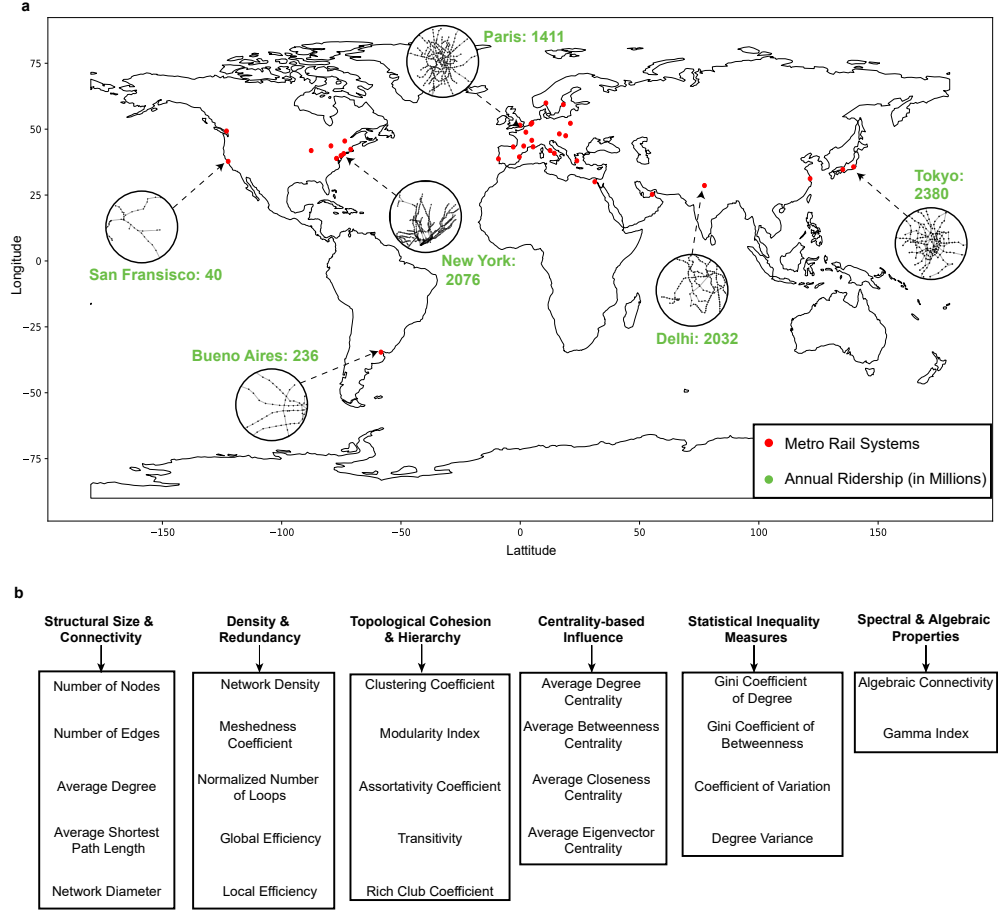


Fig. 1 Geographic distribution of 45 metro rail systems worldwide and the structural attributes used to evaluate their resilience.

(a) Geographic locations of 45 metro rail systems included in this study. Insets highlight six representative networks—Buenos Aires, Tokyo, San Francisco, New York, Paris, and Delhi—selected for their historical exposure to critical disruptions such as derailments, terrorist attacks, power failures, and sabotage. Annual ridership (in millions) is annotated in green to emphasize their socioeconomic relevance. (b) The 25 structural attributes are grouped into six categories for resilience analysis: Structural Size and Connectivity (Number of Nodes, Number of Edges, Average Degree, Average Shortest Path Length, Network Diameter), Density and Redundancy (Network Density, Meshedness Coefficient, Normalized Number of Loops, Global Efficiency, Local Efficiency), Topological Cohesion and Hierarchy (Clustering Coefficient, Modularity Index, Assortativity Coefficient, Transitivity, Rich Club Coefficient), Centrality based Influence (Average Degree Centrality, Average Betweenness Centrality, Average Closeness Centrality, Average Eigenvector Centrality), Statistical Inequality Measures (Gini Coefficient of Degree, Gini Coefficient of Betweenness, Coefficient of Variation, Degree Variance), and Spectral and Algebraic Properties (Algebraic Connectivity, Gamma Index).

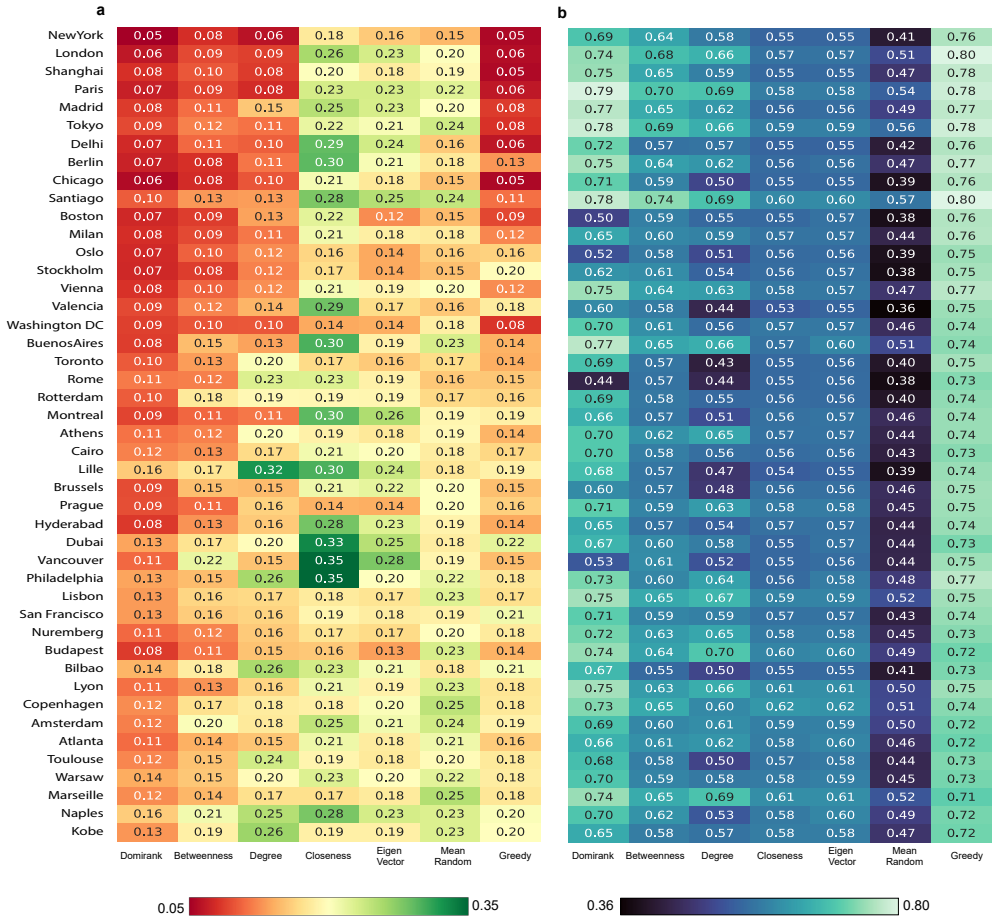


Fig. 2 Heatmap of resilience scores for 7 failure and 7 recovery strategies across 45 metro networks conveying resilience inter variability between strategies and networks. (a) Failure phase resilience scores, represented as the Area Under the Functionality Curve (AUC), for each metro network under seven node removal strategies: Domrank, Betweenness, Degree, Closeness, Eigenvector, Mean Random and Greedy Color gradients range from low (red) to high (green) resilience. (b) Recovery phase resilience scores under the same strategies, with color gradients ranging from low (dark purple) to high (turquoise green). The vertical comparison within each panel reveals how resilience varies by strategy, while the horizontal comparison across rows reflects city specific resilience patterns. Together, these panels illustrate the performance variability of intervention strategies across diverse metro topologies and urban contexts.

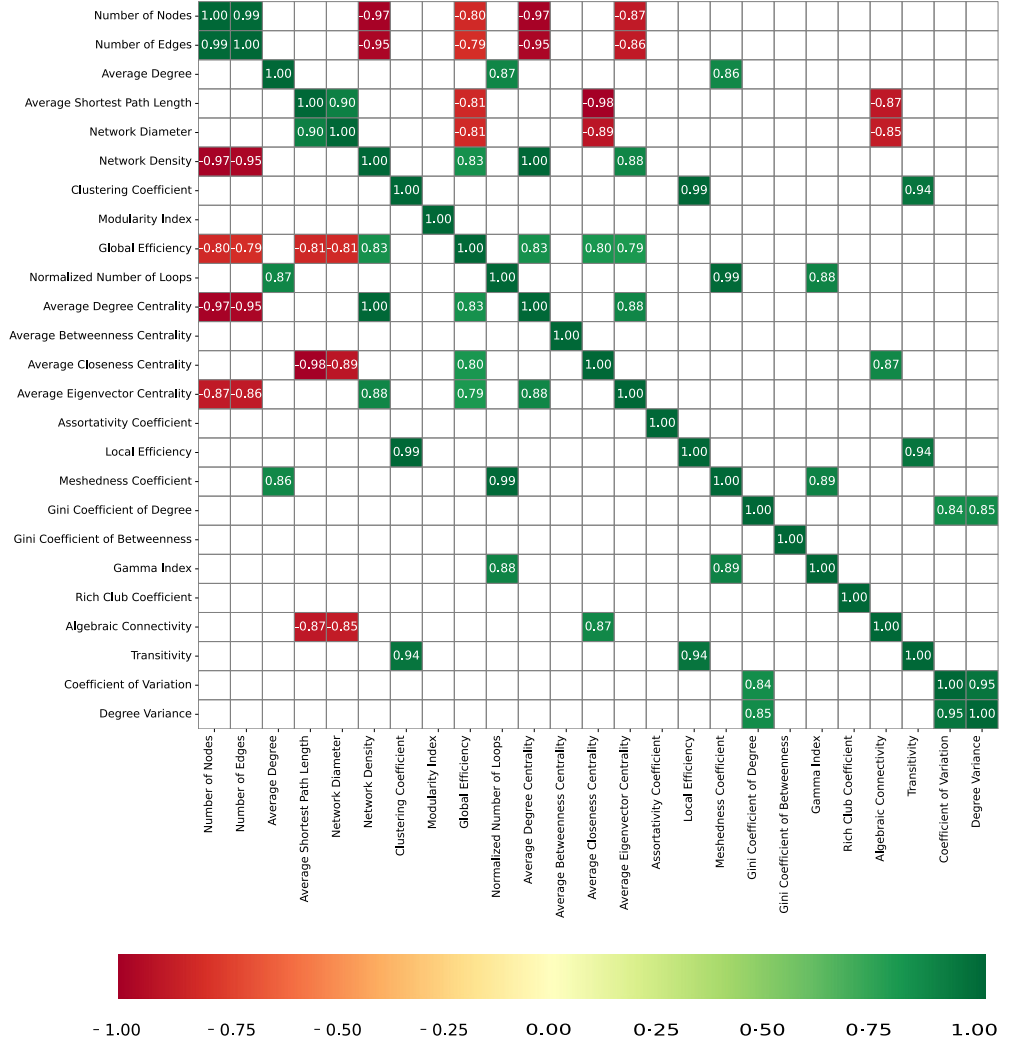


Fig. 3 A rank based (Kendall Tau) correlation plot between 25 topological network attributes indicating interdependence in information content. Kendall Tau correlation matrix among the 25 network attributes with filtered correlation pairs with absolute value greater than 0.75, highlighting potential redundancy in metrics. Color intensities in all panels range from -1 (strong negative correlation, red) to +1 (strong positive correlation, green), reinforcing the direction and strength of associations across metrics.

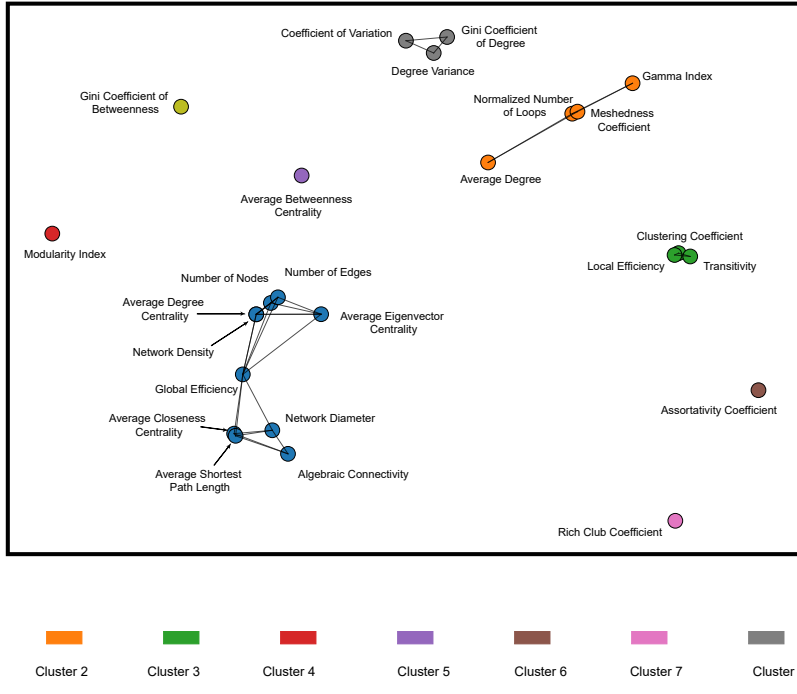


Fig. 4 Dependence structure among urban metro network attributes reveal strengths and redundancies in information content. Two dimensional map of the 25 network attributes, obtained via MDS of the Kendall–Tau dissimilarity matrix. Colours indicate clusters, where each connected component of attributes with Kendall's Tau correlation above 0.75 (positive or negative) is treated as one cluster. Edges connect attribute pairs with strong correlations, while the embedding is unit free, so only relative distances carry meaning, illustrating how attributes group into coherent structures that shape resilience.

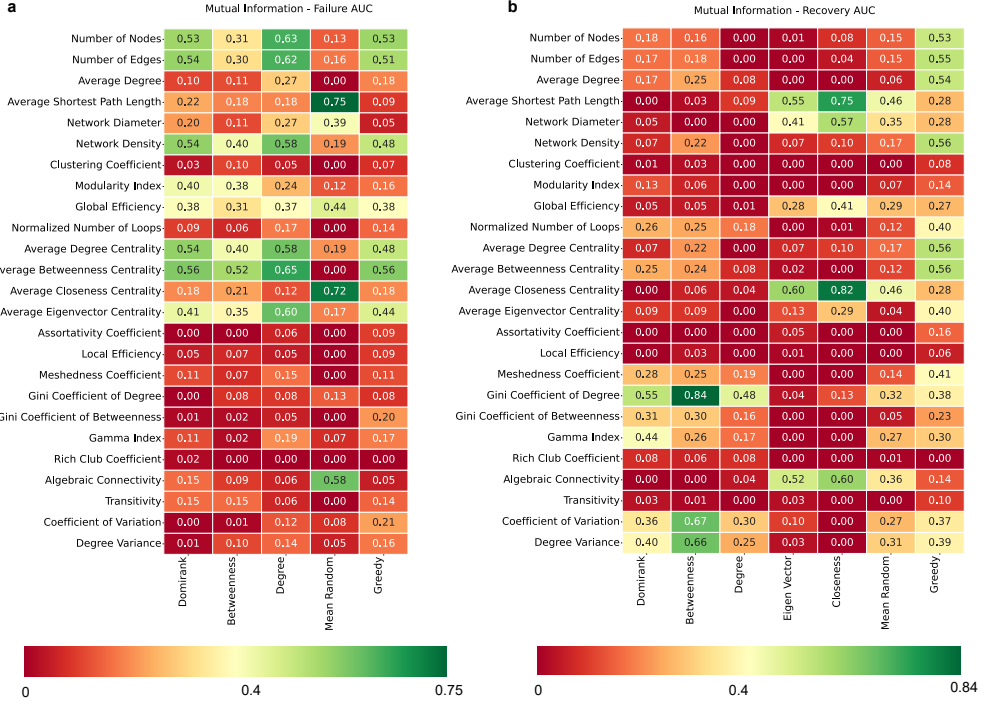


Fig. 5 Mutual information signatures of network topology and resilience scores highlight non linear dependencies. (a) Mutual information between 25 structural attributes and the AUC scores achieved by five failure strategies. (b) Mutual information between 25 structural attributes and the AUC scores achieved by seven recovery strategies. Color gradients ranging from low (red) to high (green). The vertical comparison within each panel reveals how resilience varies by strategy, while the horizontal comparison across rows reflects attribute level patterns.

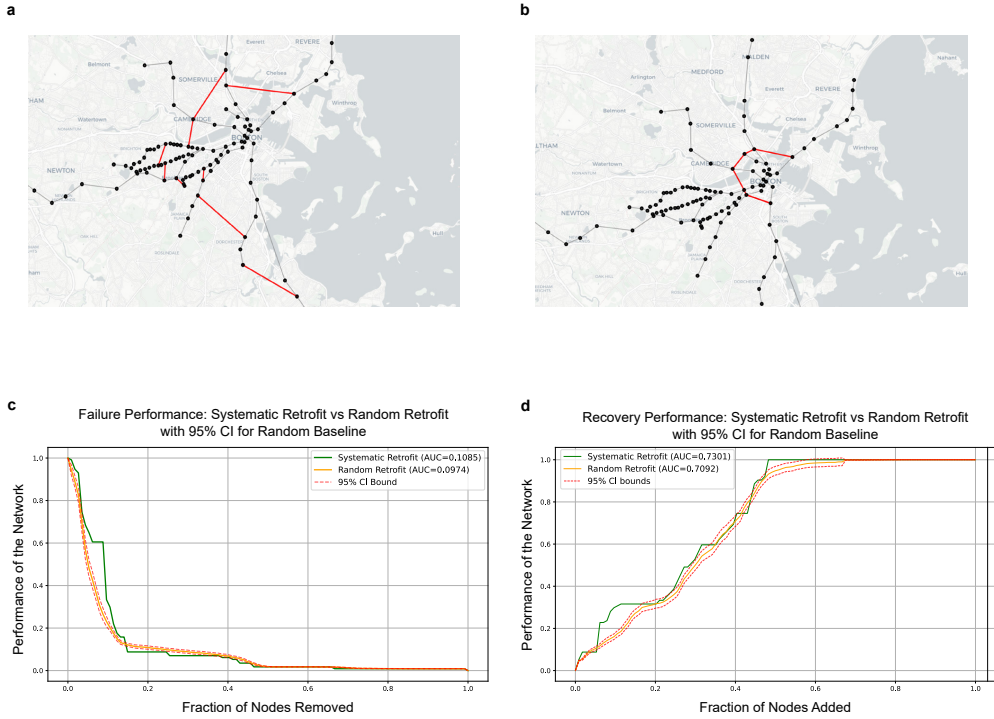


Fig. 6 Insights from 45 urban rail systems reveal that leveraging network topology informed retrofitting strategies yielded greater resilience gains in comparison to random retrofitting. (a) Spatial layout of the failure oriented retrofit: seven strategically placed links (red) bypass high betweenness hubs and strengthen peripheral redundancy. (b) Recovery oriented retrofit: a compact inner loop (red) densifies the core to accelerate reconnection after disruption. (c) Failure robustness comparison. Systematic retrofitting (green) yields an AUC = 0.1085 versus 0.0974 for random additions (orange) with 95% CI (with dashed red lines) $\approx 11.4\%$ improvement in preserved performance as nodes are removed. (d) Recovery performance comparison. The inner loop retrofit achieves an AUC = 0.7301, outperforming the random baseline (0.7092) with 95% CI (with dashed red lines) by $\approx 3\%$, indicating faster rebound as nodes are restored.

5 Algorithms and Program codes

Algorithm 1 Simulate Network Failure via Centrality-Based Node Removal

Require: Network G , Centrality strategy S (e.g., DomiRank, Betweenness, Degree), Fraction p of nodes to remove, Functionality metric $\text{Func}(\cdot)$

Ensure: Performance degradation curve F , Removal order N_S

```

1:  $G_{\text{temp}} \leftarrow G$ 
2:  $k \leftarrow \lceil p \cdot |V(G)| \rceil$ 
3: Compute centrality scores  $c(v)$  for all  $v \in V(G_{\text{temp}})$  using  $S$ 
4:  $N_S \leftarrow$  nodes sorted by  $c(v)$  in descending order (ties broken arbitrarily)
5:  $F \leftarrow [\text{Func}(G_{\text{temp}})]$ 
6: for  $i = 1$  to  $k$  do
7:    $v \leftarrow N_S[i]$ 
8:   Remove  $v$  from  $G_{\text{temp}}$ 
9:   if scores become invalid due to topology change and  $S$  is static then
10:    continue                                 $\triangleright$  Pure centrality order (no recompute)
11:   else if  $S$  is recomputed each step (optional variant) then
12:    Recompute  $c(\cdot)$  on  $G_{\text{temp}}$  and update the remaining order
13:   end if
14:   Append  $\text{Func}(G_{\text{temp}})$  to  $F$ 
15: end for
16: return  $F, N_S[1:k]$ 
```

Algorithm 2 Simulate Network Recovery via Centrality Based Node Reintroduction

Require: Original graph G_{orig} , Failed node set N_{fail} , Centrality strategy S , Functionality metric $\text{Func}(\cdot)$

Ensure: Recovery curve R , Addition order A_S

```

1:  $G_{\text{rec}} \leftarrow$  Empty graph on  $V(N_{\text{fail}})$ 
2: Compute centrality scores  $c(v)$  for all  $v \in N_{\text{fail}}$  on  $G_{\text{orig}}$  using  $S$ 
3:  $A_S \leftarrow$  nodes in  $N_{\text{fail}}$  sorted by  $c(v)$  in descending order
4:  $R \leftarrow [\text{Func}(G_{\text{rec}})]$ 
5: for each  $v$  in  $A_S$  do
6:   Add  $v$  to  $G_{\text{rec}}$  and restore all incident edges from  $G_{\text{orig}}$  whose other endpoints
      are already present in  $G_{\text{rec}}$ 
7:   Append  $\text{Func}(G_{\text{rec}})$  to  $R$ 
8: end for
9: return  $R, A_S$ 
```

Algorithm 3 Greedy Based Failure via Iterative Node Removal

Require: Network G , Fraction p of nodes to remove, Functionality metric $\text{Func}(\cdot)$
Ensure: Performance degradation curve F , Removal order N_{greedy}

```
1:  $G_{\text{temp}} \leftarrow G$ ;  $F \leftarrow [\text{Func}(G_{\text{temp}})]$ ;  $N_{\text{greedy}} \leftarrow []$ 
2:  $k \leftarrow \lceil p \cdot |V(G)| \rceil$ 
3: while  $|N_{\text{greedy}}| < k$  and  $V(G_{\text{temp}}) \neq \emptyset$  do
4:   for each  $v \in V(G_{\text{temp}})$  do
5:     Temporarily remove  $v$  from  $G_{\text{temp}}$  to obtain  $G^{-v}$ 
6:      $\Delta(v) \leftarrow \text{Func}(G_{\text{temp}}) - \text{Func}(G^{-v})$  ▷ Immediate drop
7:     Restore  $v$  to  $G_{\text{temp}}$ 
8:   end for
9:    $v^* \leftarrow \arg \max_v \Delta(v)$  ▷ Largest immediate damage
10:  Permanently remove  $v^*$ ; append  $v^*$  to  $N_{\text{greedy}}$ 
11:  Append  $\text{Func}(G_{\text{temp}})$  to  $F$ 
12: end while
13: return  $F, N_{\text{greedy}}$ 
```

Algorithm 4 Greedy Based Recovery via Iterative Node Reintroduction

Require: Original graph G_{orig} , Failed node set N_{fail} , Functionality metric $\text{Func}(\cdot)$
Ensure: Recovery curve R , Addition order A_{greedy}

```
1:  $G_{\text{rec}} \leftarrow$  Empty graph on  $V(N_{\text{fail}})$ 
2:  $R \leftarrow [\text{Func}(G_{\text{rec}})]$ ;  $A_{\text{greedy}} \leftarrow []$ ;  $U \leftarrow N_{\text{fail}}$ 
3: while  $U \neq \emptyset$  do
4:   for each  $v \in U$  do
5:     Let  $G^{+v}$  be  $G_{\text{rec}}$  with  $v$  added and all original incident edges from  $G_{\text{orig}}$  to
       nodes already in  $G_{\text{rec}}$ 
6:      $\Delta(v) \leftarrow \text{Func}(G^{+v}) - \text{Func}(G_{\text{rec}})$  ▷ Immediate gain
7:   end for
8:    $v^* \leftarrow \arg \max_{v \in U} \Delta(v)$  ▷ Largest immediate improvement
9:    $G_{\text{rec}} \leftarrow G^{+v^*}$ ; append  $v^*$  to  $A_{\text{greedy}}$ ;  $U \leftarrow U \setminus \{v^*\}$ 
10:  Append  $\text{Func}(G_{\text{rec}})$  to  $R$ 
11: end while
12: return  $R, A_{\text{greedy}}$ 
```

Algorithm 5 Mean Random Failure via Uniform Node Removal

Require: Network G , Fraction p of nodes to remove, Functionality metric $\text{Func}(\cdot)$, Number of trials $T = 50$

Ensure: Mean performance degradation curve \bar{F} , 95% confidence interval CI_F

- 1: $k \leftarrow \lceil p \cdot |V(G)| \rceil$; Initialize accumulator $\mathcal{F} \leftarrow []$
- 2: **for** $t = 1$ **to** T **do**
- 3: $G_{\text{temp}} \leftarrow G$
- 4: $order \leftarrow$ random permutation of $V(G)$
- 5: $F^{(t)} \leftarrow [\text{Func}(G_{\text{temp}})]$
- 6: **for** $i = 1$ **to** k **do**
- 7: Remove $order[i]$ from G_{temp}
- 8: Append $\text{Func}(G_{\text{temp}})$ to $F^{(t)}$
- 9: **end for**
- 10: Append $F^{(t)}$ to \mathcal{F}
- 11: **end for**
- 12: $\bar{F} \leftarrow$ elementwise mean over all curves in \mathcal{F}
- 13: $\text{CI}_F \leftarrow$ elementwise $1.96 \times \frac{\sigma}{\sqrt{T}}$ where σ is the sample standard deviation across runs
- 14: **return** \bar{F}, CI_F

Algorithm 6 Mean Random Recovery via Uniform Node Reintroduction

Require: Original graph G_{orig} , Failed node set N_{fail} , Functionality metric $\text{Func}(\cdot)$, Number of trials $T = 50$

Ensure: Mean recovery curve \bar{R} , 95% confidence interval CI_R

- 1: Initialize accumulator $\mathcal{R} \leftarrow []$
- 2: **for** $t = 1$ **to** T **do**
- 3: $G_{\text{rec}} \leftarrow$ Empty graph on $V(N_{\text{fail}})$
- 4: $order \leftarrow$ random permutation of N_{fail}
- 5: $R^{(t)} \leftarrow [\text{Func}(G_{\text{rec}})]$
- 6: **for each** v in $order$ **do**
- 7: Add v to G_{rec} and restore all original edges from G_{orig} whose other endpoints are already in G_{rec}
- 8: Append $\text{Func}(G_{\text{rec}})$ to $R^{(t)}$
- 9: **end for**
- 10: Append $R^{(t)}$ to \mathcal{R}
- 11: **end for**
- 12: $\bar{R} \leftarrow$ elementwise mean over all curves in \mathcal{R}
- 13: $\text{CI}_R \leftarrow$ elementwise $1.96 \times \frac{\sigma}{\sqrt{T}}$ where σ is the sample standard deviation across runs
- 14: **return** \bar{R}, CI_R

Declarations

- **Funding**

This research was primarily supported by the U.S. Department of Defense (US DOD) Strategic Environmental Research and Development Program (SERDP) project number RC20-1183 titled Networked Infrastructures under Compound Extremes (NICE). Partial funding was provided by the US Department of Homeland Security (DHS) and by Northeastern University through the AI for Climate and Sustainability (AI4CaS) focus area of the Institute for Experiential AI (EAI).

- **Conflict of interest/Competing interests**

The authors declare no competing interests.

- **Ethics approval and consent to participate**

Not applicable.

- **Consent for publication**

All authors have reviewed and approved the final version of the manuscript and consent to its publication.

- **Data availability**

We complemented our curated railway topology dataset with publicly available networks from [17]. The complete dataset used in this study (original sources and our additions) is openly available at https://github.com/orijeet100/urban_rail_research..

- **Materials availability**

Not applicable.

- **Code availability**

All code required to reproduce this study—failure and recovery simulations, computation of 25 topological attributes, information-theoretic screening and clustering, and figure/table generation is openly available at https://github.com/orijeet100/urban_rail_research..

- **Author contribution**

O.M. and A.G. conceptualized and formulated the problem. O.M led the study, conducted all simulations, data acquisition and statistical analyses. O.M. prepared the manuscript primarily with A.G. and D.Z., A.P. and J.W. contributed domain knowledge. M.G., S.C., and A.G. provided guidance, reviewed the work critically, and helped shape the study direction.

- **Correspondence Email**

To whom correspondence should be addressed; E-mail: a.ganguly@northeastern.edu.

Supplementary Material

Extended Figures

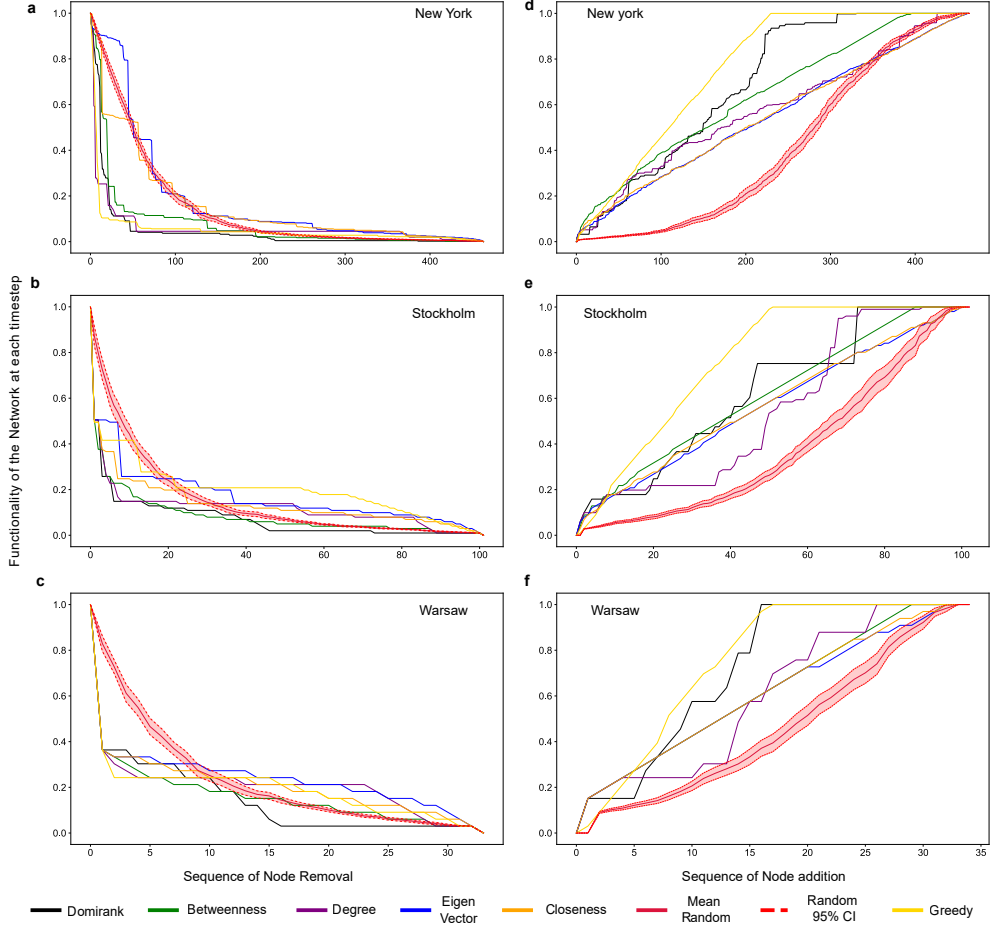


Fig. A1 Resilience performance curves under node failure and recovery strategies. Panels (a–c) show how the network functionality degrades with sequential node removals across three cities of varying scale: New York (large), Stockholm (medium), and Warsaw (small). Panels (d–f) illustrate the corresponding recovery sequences, where nodes are reintroduced in different orders. Each line represents a distinct strategy—centrality based (Domirank, Betweenness, Degree, Eigen Vector), Mean Random and Greedy attacks and recovery. These patterns emphasize the varying impacts of sequence of node removal on both fragility and restoration potential across urban systems. The red dashed line denotes the average performance of 50 random simulations, with the surrounding shaded band indicating the 95% confidence interval. These examples highlight how resilience trajectories vary by both strategy and underlying network structure.

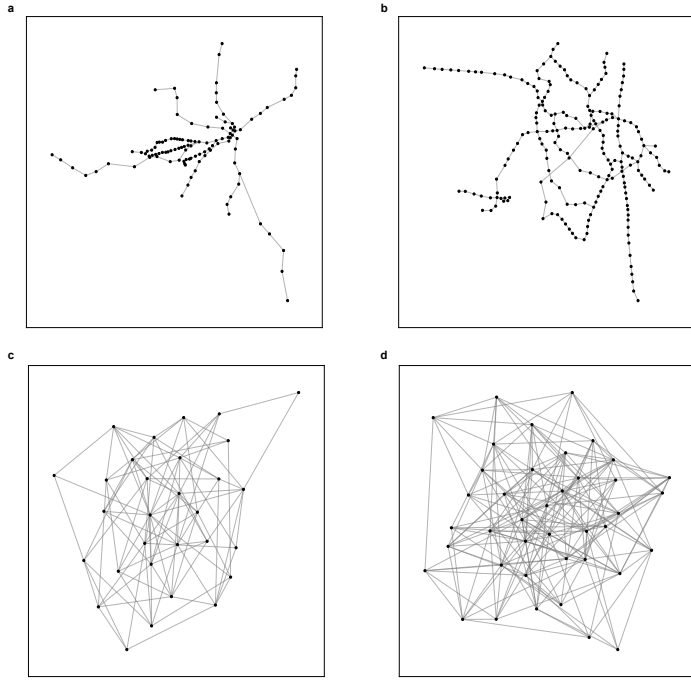


Fig. A2 Real World vs. Synthetic High Density Metro Networks. (a) Boston and (b) Delhi metro networks visualized using geospatial coordinates to reflect their true layout and branching topology. (c) and (d) show two synthetic, densely connected graphs generated using the Erdős–Rényi model.

Mutual Information - Failure AUC (including Eigen Vector and Closeness)



Fig. A3 Mutual information heat map of topology attributes versus failure AUC including Eigenvector and Closeness based strategies. Mutual information between 25 structural attributes and AUC scores for all failure strategies including the Eigen vector and Closeness guided failures. Virtually all scores in these two columns fall below 0.20 (deep red), indicating negligible explanatory power compared with the other five strategies. Owing to this consistently low signal, Eigenvector and Closeness based failures were excluded from the main comparative analysis.

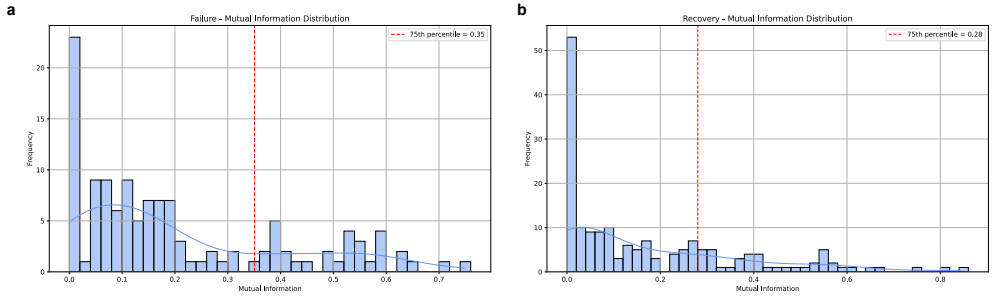


Fig. A4 Distributions of mutual information scores and selection threshold for high mutual information attributes. (a) Distribution of mutual information values between topology attributes and failure AUC. The red dashed line marks the 75th percentile threshold (mutual information=0.35); only attributes to the right of this cutoff are retained as failure relevant.(b) Distribution of mutual information values for recovery AUC. The 75th percentile cutoff (mutual information = 0.28) isolates the top quartile of information rich attributes used in the recovery analysis.

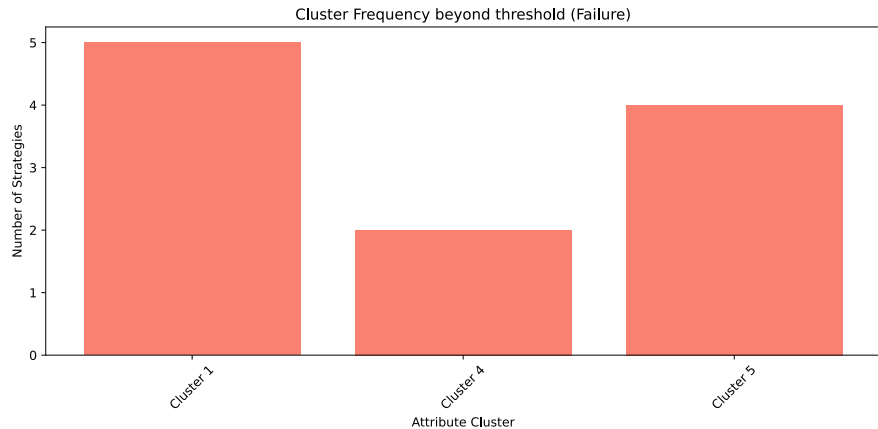
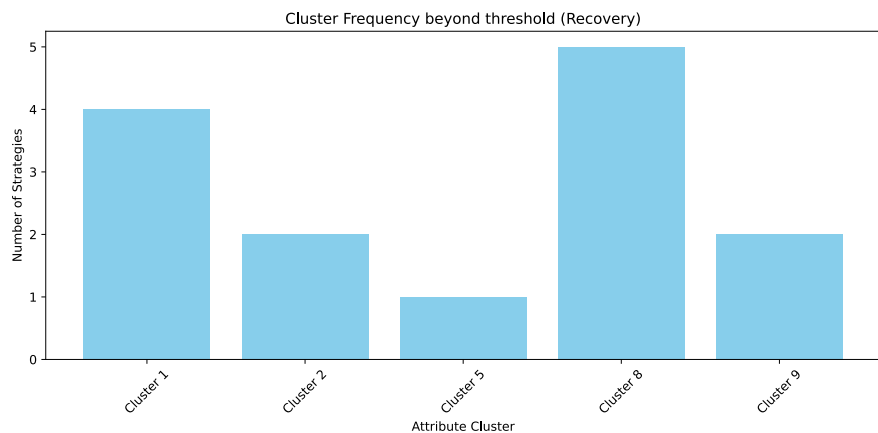
a**b**

Fig. A5 Frequency of attribute cluster occurrence above the high mutual information threshold across failure and recovery strategies (a) Failure strategies ($n = 5$). Bars show, for each attribute cluster, the number of failure strategies in which the cluster appears at least once above the 75th percentile mutual information threshold. (b) Recovery strategies ($n = 7$). Bars show, for each attribute cluster, the number of recovery strategies in which the cluster appears at least once above the 75th percentile mutual information threshold

Extended Tables

Table A1 Network attributes used across resilience studies in urban rail transit networks. Each "✓" indicates the attribute is used in the corresponding study.

Attributes	[24]	[3]	[25]	[26]	[17]	[5]	[27]	[6]	[4]	[28]	[29]	[10]	[30]	[31]	[32]	[33]	[34]	[35]	[36]	[37]	[38]
Number of Nodes					✓					✓				✓	✓	✓	✓	✓	✓	✓	
Number of Edges					✓					✓				✓	✓	✓	✓	✓	✓	✓	
Average Degree	✓									✓	✓			✓	✓	✓	✓		✓	✓	
Average Shortest Path Length	✓				✓	✓		✓	✓	✓	✓		✓	✓	✓	✓	✓	✓			
Network Diameter			✓	✓	✓	✓				✓	✓			✓	✓			✓			
Network Density						✓														✓	
Clustering Coefficient	✓					✓		✓	✓				✓	✓	✓					✓	
Modularity Index											✓										
Global Efficiency	✓	✓										✓	✓	✓	✓	✓	✓	✓	✓		
Normalized Number of Loops				✓						✓											
Average Degree Centrality			✓			✓			✓	✓	✓	✓	✓							✓	
Average Betweenness Centrality	✓		✓	✓	✓	✓		✓	✓	✓	✓	✓	✓	✓	✓	✓	✓	✓			
Average Closeness Centrality			✓			✓														✓	
Average Eigenvector Centrality			✓			✓					✓						✓			✓	
Assortativity Coefficient		✓	✓																		
Local Efficiency					✓																
Mesherdness Coefficient				✓															✓		
Gini Coefficient of Degree																				✓	
Gini Coefficient of Betweenness																				✓	
Gamma Index																				✓	
Rich Club Coefficient																				✓	
Algebraic Connectivity																					
Transitivity																					
Coefficient of Variation																					
Degree Variance																					

Table A2 Presence of high-mutual-information clusters for **failure** and **recovery** strategies. An “✓” marks each attribute cluster that appears above the 75th-percentile MI threshold for the given strategy.

Strategies	C1	C2	C3	C4	C5	C6	C7	C8	C9
Domirank Failure	✓		✓	✓					
Betweenness Failure	✓			✓	✓				
Degree Failure	✓				✓				
Mean Random Failure	✓								
Greedy Failure	✓					✓			
Domirank Recovery		✓					✓	✓	
Betweenness Recovery							✓	✓	
Degree Recovery							✓		
Eigen Vector Recovery	✓								
Closeness Recovery	✓								
Mean Random Recovery	✓							✓	
Greedy Recovery	✓	✓			✓			✓	

References

- [1] Zhenhua Chen, Y.W.: Impacts of severe weather events on high-speed rail and aviation delays. *Transportation Research Part D: Transport and Environment* **69**, 168–183 (2019) <https://doi.org/10.1016/j.trd.2019.01.030>
- [2] Abigail Luxton, M.M.: Terrorist threat mitigation strategies for the railways. *Sustainability* **12**(8), 3408 (2020) <https://doi.org/10.3390/su12083408>
- [3] Dong, T., Li, Y., Sun, K., Chen, J.: Research on the resilience of a railway network based on a complex structure analysis of physical and service networks. *Applied Sciences* **15**(9), 5135 (2025) <https://doi.org/10.3390/app15095135>
- [4] Saadat, Y., Ayyub, B.M., Zhang, Y., Zhang, D., Huang, H.: Resilience of metrorail networks: Quantification with washington, dc as a case study. *ASCE-ASME J Risk and Uncert in Engng Sys Part B Mech Engrg* **5**(4) (2019) <https://doi.org/10.1115/1.4044038>
- [5] Mattsson, L.-G., Jenelius, E.: Vulnerability and resilience of transport systems – a discussion of recent research. *Transportation Research Part A: Policy and Practice* **81**, 16–34 (2015) <https://doi.org/10.1016/j.tra.2015.06.002>
- [6] Ma, Y., Sallan, J.M., Lordan, O.: Motif analysis of urban rail transit network. *Physica A: Statistical Mechanics and its Applications* **625**, 129016 (2023) <https://doi.org/10.1016/j.physa.2023.129016>
- [7] Luo, D., Cats, O., Lint, H., Currie, G.: Integrating network science and public transport accessibility analysis for comparative assessment. *Journal of Transport Geography* **80**, 102505 (2019) <https://doi.org/10.1016/j.jtrangeo.2019.102505>

- [8] Serdar, M.Z., Koç, M., Al-Ghamdi, S.G.: Urban transportation networks resilience: Indicators, disturbances, and assessment methods. *Sustainable Cities and Society* **76**, 103452 (2022) <https://doi.org/10.1016/j.scs.2021.103452>
- [9] Bešinović, N.: Resilience in railway transport systems: a literature review and research agenda. *Transport Reviews* **40**(4), 457–478 (2020) <https://doi.org/10.1080/01441647.2020.1728419>
- [10] Yadav, N., Chatterjee, S., Ganguly, A.R.: Resilience of urban transport network-of-networks under intense flood hazards exacerbated by targeted attacks. *Scientific Reports* **10**(1) (2020) <https://doi.org/10.1038/s41598-020-66049-y>
- [11] Pagani, A., Mosquera, G., Alturki, A., Johnson, S., Jarvis, S., Wilson, A., Guo, W., Varga, L.: Resilience or robustness: identifying topological vulnerabilities in rail networks. *Royal Society Open Science* **6**(2), 181301 (2019) <https://doi.org/10.1098/rsos.181301>
- [12] Xu, P.-C., Lu, Q.-C., Xie, C., Cheong, T.: Modeling the resilience of interdependent networks: The role of function dependency in metro and bus systems. *Transportation Research Part A: Policy and Practice* **179**, 103907 (2024) <https://doi.org/10.1016/j.tra.2023.103907>
- [13] Tube strike: commuters struggle in worst disruption for 13 years — London Underground — The Guardian (2025). <https://www.theguardian.com/uk-news/2015/jul/09/tube-strike-london-commuters-chaos-rail-bus-trains>
- [14] Tohoku Earthquake — The Geological Society of London (2025). <https://www.geolsoc.org.uk/science-and-policy/plate-tectonic-stories/tohoku-earthquake/>
- [15] Hosseini, S., Barker, K., Ramirez-Marquez, J.E.: A review of definitions and measures of system resilience. *Reliability Engineering and System Safety* **145**, 47–61 (2016) <https://doi.org/10.1016/j.ress.2015.08.006>
- [16] Jack R. Watson, A.G. Samrat Chatterjee: Resilience of urban rail transit networks under compound natural and opportunistic failures. *2022 IEEE International Symposium on Technologies for Homeland Security (HST)*, 1–8 (2022) <https://doi.org/10.1109/hst56032.2022.10025456>
- [17] Massobrio, R., Cats, O.: Topological assessment of recoverability in public transport networks. *Communications Physics* **7**(1) (2024) <https://doi.org/10.1038/s42005-024-01596-8>
- [18] Argentina Train Crash in Buenos Aires Kills 49 - BBC News. <https://www.bbc.com/news/world-latin-america-17129858>
- [19] Okumura, T., Suzuki, K., Fukuda, A., Kohama, A., Takasu, N., Ishimatsu, S.,

- Hinohara, S.: The tokyo subway sarin attack: Disaster management, part 1: Community emergency response. Academic Emergency Medicine **5**(6), 613–617 (1998) <https://doi.org/10.1111/j.1553-2712.1998.tb02470.x>
- [20] Murphy, G.K.: Death in the desert: The sabotage-derailment of “the city of san francisco”. The American Journal of Forensic Medicine and Pathology **4**(2), 145–148 (1983) <https://doi.org/10.1097/00000433-198306000-00009>
- [21] Caramela, S.: 3,500 NYC Commuters Were Trapped on the Subway With No Service, No AC. <https://www.vice.com/en/article/nyc-commuters-trapped-subway-no-service-no-ac>
- [22] Who Launched Attack on the French Rail Network – and Why? — France — The Guardian. <https://www.theguardian.com/world/article/2024/jul/26/who-launched-attack-on-the-french-rail-network-and-why>
- [23] Chronology of blasts in Delhi - The Hindu (2025). <https://www.thehindu.com/news/national/chronology-of-blasts-in-delhi/article2432097.ece>
- [24] Wei, Y., Yang, X., Xiao, X., Ma, Z., Zhu, T., Dou, F., Wu, J., Chen, A., Gao, Z.: Understanding the resilience of urban rail transit: Concepts, reviews, and trends. Engineering **41**, 7–18 (2024) <https://doi.org/10.1016/j.eng.2024.01.022>
- [25] Wang, Y., Liu, J., Li, Z.: The resilience of an urban rail transit network: An evaluation approach based on a weighted coupled map lattice model. Mathematics **13**(4), 608 (2025) <https://doi.org/10.3390/math13040608>
- [26] Qi, Q., Meng, Y., Zhao, X., Liu, J.: Resilience assessment of an urban metro complex network: A case study of the zhengzhou metro. Sustainability **14**(18), 11555 (2022) <https://doi.org/10.3390/su141811555>
- [27] Bhatia, U., Kumar, D., Kodra, E., Ganguly, A.R.: Network science based quantification of resilience demonstrated on the indian railways network. PLOS ONE **10**(11), 0141890 (2015) <https://doi.org/10.1371/journal.pone.0141890>
- [28] Lin, J., Ban, Y.: Complex network topology of transportation systems. Transport Reviews **33**(6), 658–685 (2013) <https://doi.org/10.1080/01441647.2013.848955>
- [29] Derrible, S., Kennedy, C.: The complexity and robustness of metro networks. Physica A: Statistical Mechanics and its Applications **389**(17), 3678–3691 (2010) <https://doi.org/10.1016/j.physa.2010.04.008>
- [30] Xu, Z., Chopra, S.S.: Interconnectedness enhances network resilience of multimodal public transportation systems for safe-to-fail urban mobility. Nature Communications **14**(1) (2023) <https://doi.org/10.1038/s41467-023-39999-w>
- [31] Bhatia, U., Sela, L., Ganguly, A.R.: Hybrid method of recovery: Combining

- topology and optimization for transportation systems. *Journal of Infrastructure Systems* **26**(3) (2020) [https://doi.org/10.1061/\(asce\)is.1943-555x.0000566](https://doi.org/10.1061/(asce)is.1943-555x.0000566)
- [32] Xu, C., Xu, X.: A two-stage resilience promotion approach for urban rail transit networks based on topology enhancement and recovery optimization. *Physica A: Statistical Mechanics and its Applications* **635**, 129496 (2024) <https://doi.org/10.1016/j.physa.2024.129496>
 - [33] Saadat, Y., Ayyub, B.M., Zhang, Y., Zhang, D., Huang, H.: Resilience-based strategies for topology enhancement and recovery of metrorail transit networks. *ASCE-ASME Journal of Risk and Uncertainty in Engineering Systems, Part A: Civil Engineering* **6**(2) (2020) <https://doi.org/10.1061/ajrua6.0001057>
 - [34] Cats, O.: Topological evolution of a metropolitan rail transport network: The case of stockholm. *Journal of Transport Geography* **62**, 172–183 (2017) <https://doi.org/10.1016/j.jtrangeo.2017.06.002>
 - [35] Liu, C., Su, X., Wu, Z., Zhang, Y., Zhou, C., Wu, X., Huang, Y.: Exploration of the mountainous urban rail transit resilience under extreme rainfalls: A case study in chongqing, china. *Applied Sciences* **15**(2), 735 (2025) <https://doi.org/10.3390/app15020735>
 - [36] Wen He, J.-J.C. Yue Pan: Enhanced metro resilience assessment combining dynamic cascade-based simulation and deep learning-based attributed graph clustering. *IEEE Transactions on Intelligent Transportation Systems*, 1–17 (2025) <https://doi.org/10.1109/tits.2025.3572111>
 - [37] Ming Li, H.W. Hongwei Wang: Resilience assessment and optimization for urban rail transit networks: A case study of beijing subway network. *IEEE Access* **7**, 71221–71234 (2019) <https://doi.org/10.1109/access.2019.2919105>
 - [38] Zhang, Y., Ng, S.T.: Unveiling the rich-club phenomenon in urban mobility networks through the spatiotemporal characteristics of passenger flow. *Physica A: Statistical Mechanics and its Applications* **584**, 126377 (2021) <https://doi.org/10.1016/j.physa.2021.126377>
 - [39] Xu, X., Xu, C., Zhang, W.: Research on the destruction resistance of giant urban rail transit network from the perspective of vulnerability. *Sustainability* **14**(12), 7210 (2022) <https://doi.org/10.3390/su14127210>
 - [40] Engsig, M., Tejedor, A., Moreno, Y., Foufoula-Georgiou, E., Kasmi, C.: Domi-rank centrality reveals structural fragility of complex networks via node dominance. *Nature Communications* **15**(1) (2024) <https://doi.org/10.1038/s41467-023-44257-0>
 - [41] Kendall, M.G.: A new measure of rank correlation. *Biometrika* **30**(1/2), 81–93 (1938) <https://doi.org/10.2307/2332226>

- [42] Dormann, C.F., Elith, J., Bacher, S., Buchmann, C., Carl, G., Carré, G., Marquéz, J.R.G., Gruber, B., Lafourcade, B., Leitão, P.J., Münkemüller, T., McClean, C., Osborne, P.E., Reineking, B., Schröder, B., Skidmore, A.K., Zurell, D., Lautenbach, S.: Collinearity: a review of methods to deal with it and a simulation study evaluating their performance. *Ecography* **36**(1), 27–46 (2012) <https://doi.org/10.1111/j.1600-0587.2012.07348.x>
- [43] Kruskal, J.B.: Multidimensional scaling by optimizing goodness of fit to a non-metric hypothesis. *Psychometrika* **29**(1), 1–27 (1964) <https://doi.org/10.1007/bf02289565>
- [44] Ross, B.C.: Mutual information between discrete and continuous data sets. *PLoS ONE* **9**(2), 87357 (2014) <https://doi.org/10.1371/journal.pone.0087357>
- [45] Cheng, J., Sun, J., Yao, K., Xu, M., Cao, Y.: A variable selection method based on mutual information and variance inflation factor. *Spectrochimica Acta Part A: Molecular and Biomolecular Spectroscopy* **268**, 120652 (2022) <https://doi.org/10.1016/j.saa.2021.120652>
- [46] Ouyang, M., Dueñas-Osorio, L.: Time-dependent resilience assessment and improvement of urban infrastructure systems. *Chaos: An Interdisciplinary Journal of Nonlinear Science* **22**(3) (2012) <https://doi.org/10.1063/1.4737204>
- [47] Ganin, A.A., Kitsak, M., Marchese, D., Keisler, J.M., Seager, T., Linkov, I.: Resilience and efficiency in transportation networks. *Science Advances* **3**(12) (2017) <https://doi.org/10.1126/sciadv.1701079>
- [48] Ma, Z., Yang, X., Chen, A., Zhu, T., Wu, J.: Assessing the resilience of multi-modal transportation networks with the integration of urban air mobility. *Transportation Research Part A: Policy and Practice* **195**, 104465 (2025) <https://doi.org/10.1016/j.tra.2025.104465>
- [49] Pregnolato, M., Ford, A., Glenis, V., Wilkinson, S., Dawson, R.: Impact of climate change on disruption to urban transport networks from pluvial flooding. *Journal of Infrastructure Systems* **23**(4) (2017) [https://doi.org/10.1061/\(asce\)is.1943-555x.0000372](https://doi.org/10.1061/(asce)is.1943-555x.0000372)